Materials Research. 2017; 20(6): 1713-1721
DOI: http://dx.doi.org/10.1590/1980-5373-MR-2017-0467

Morphological Characterization of Tungsten Trioxide Nanopowders Synthesized by Sol-Gel Modified Pechini's Method

Leila Ghasemi[a], Hassan Jafari[a]*

[a]Department of Materials Engineering, Faculty of Mechanical Engineering, Shahid Rajaee Teacher Training University, 16785-136, Tehran, Iran

Received: May 04, 2017; Revised: August 07, 2017; Accepted: August 27, 2017

Sol-gel modified Pechini's method was used to prepare WO_3 nanopowders using dicarboxylic acid and polyethylene glycol as the chelating agent and polymeric source, respectively. WO_3 powders were first prepared by calcination of resin precursor at 550ºC under various initial concentrations of metal ion (12.5-50 mmol), acid (125-500 mmol), a complexing agent (32-262 mmol), and polyethylene glycol (1-16.5 mmol) in the air atmosphere. The products were characterized using X-ray powder diffraction, field emission scanning electron microscopy, and energy dispersive spectroscopy. The results revealed that the WO_3 nanopowders prepared with different amounts of chelating agent and polyethylene glycol, crystallized in monoclinic phase. The nanopowders were impurity-free due to the presence of the complexing agent and polyethylene glycol as carbon sources. Morphological evolution indicated that the nanopowders evolved from rod-like to regular and spherical shapes, depending on complexing agent and polyethylene glycol amounts. Nanopowders with an average particle size of approximately 58 nm and a narrow size distribution were obtained.

Keywords: *Tungsten trioxide, Nanomaterials, Sol-gel, Morphology, Pechini.*

1. Introduction

Tungsten trioxide (WO_3) as one of the most interesting material in the fields of material science and metallurgy is used in various industrial applications. WO_3 films are utilized in electrochromic devices, photocatalysis, and gas sensors[1-3]. In addition, the production of tungsten powder from high purity WO_3 through hydrogen reduction is still the most important application in the field of powder metallurgy[4]. More important, it has been confirmed that nanostructured WO_3 exhibits improved properties in comparison to the conventional coarse-grained structures. This is believed to result from the greatly increased surface area, which provides a large interface between the solid and a gaseous or liquid medium to react[5,6].

Nowadays, nanopowders are produced by using different physical, mechanical, and chemical methods. Among the chemical processes, the sol-gel technique is known as a very simple and inexpensive approach in which shape and size of powder can successfully be controlled[7]. This technique uses three main routes for preparing metal oxides. The routes include (1) hydrolysis and condensation of metal alkoxides; (2) gel making of aqueous solutions contain metal-chelates; and (3) esterification reaction between carboxylic acids (acetic, formic, oxalic) and polymer molecules (ethylene glycol) also known as the Pechini's method[8,9]. This method is known as a simple approach for preparing metal oxide powders where polymeric precursors are made from metal salts, ethylene glycol, and citric acid during a low-temperature heat treatment. The main advantage of this approach is that metal ions are often mixed in atomic level, resulting in an increase in reaction rate. In this method of powder preparation, two reactions occur: at first complex formation between citric acid and metals, and subsequently esterification between citric acid and ethylene glycol (EG). As a result, the polymeric organic net formed by the esterification reaction decreases the ion segregation[10]. Many researchers have studied powder preparation of WO_3 by sol-gel method[11-15]. Han et al.[15] reported that nanometric WO_3 powders with uniform size and spherical shape can be synthesized in the presence of oxalic acid and cetyltrimethyl ammonium bromide as the complexing and surface active agents, respectively. Results of the investigations revealed that the morphological characteristics of the powder like particle size and shape depend strongly on the preparation conditions such as nature of precursor, solvent, the surface modifier and quantities of them. To the best of author's knowledge, the application of sol-gel modified Pechini's method in the usage of sodium tungstate solution (Na_2WO_4) and oxalic acid as the precursor and chelating agent, respectively, to prepare of WO_3 nanopowder has not been previously reported. Oxalic acid has been reported to have a better complexing effect than monofunctional citric acid[15], therefore it was selected to be used in the present investigation. The sol-gel modified Pechini's method was applied to produce nanosized WO_3 using sodium tungstate dehydrated ($Na_2WO_4.2H_2O$) as the starting material. Although there are other starting materials such as alkoxides, which are very common in use

*e-mail: jafari_h@yahoo.com

in the sol-gel method, there are some disadvantages in the case of tungsten alkoxide precursors. These materials not only are not easily available; but also storing and handling of these materials are difficult due to their high chemical reactivity and sensitivity to moisture. In contrast, the alkaline precursor is inexpensive and easily accessible[14]. This study mainly aimed at evaluating the morphology and size of the WO_3 nanopowders synthesized by the sol-gel modified Pechini's method.

2. Material and Methods

2.1 Preparation of resin precursor

Sodium tungstate dehydrates ($Na_2WO_4.2H_2O$, 99.99%, Merck) powder as the starting material, and hydrochloric acid (HCl, 37%, Merck) as well as nitric acid (HNO_3, 68%, Merck) as the chemical materials for ion exchange reaction, were used during the research. Oxalic acid dihydrate powder ($H_2C_2O_4.2H_2O$, 99.99%, Merck) and polyethylene glycol with a chain length of 200 (PEG 200, 99.99%, Merck) were used as the complexing agent and polymeric source, respectively. Deionized water was used for solution preparation and washing steps. All the chemicals and solvents were used without further purifications. The $Na_2WO_4.2H_2O$ powder was dissolved in water, according to Table 1, then heated at 80ºC. This table summarizes the preparation conditions for the experiments. Next, a mixture of HCl and HNO_3 (molar ratio of 1:1) was added to the solution at the same temperature, while it was being stirred, to adjust the pH to 1-2 and enhance ion exchange process. After a while, the yellow precipitate was formed and converted into a soft gel through aging. Then the gel was washed by the addition of hot distilled water or 0.1 N HCl solution to the gel followed by stirring and aging the soft gel at the same temperature. Several washing steps were applied to remove residual acid and by-products of the reaction. Oxalic acid and PEG were then added as chelating and resin agents, respectively. Finally, the WO_3 nanoparticles were synthesized by heat treatment of resin precursor prepared from hydrated tungstic precipitates. The samples were first heated at 150 ºC to remove residual water, then heated to 550 ºC, and kept at this temperature for 90 min followed by cooling to room temperature.

2.2 Characterization

The particles in the samples were dispersed using ultrasonic separation. The structural characterization of the powder products was conducted using X-ray diffraction (Philips by a K_{Cu} source with a wavelength of 1.54056 Aº). The morphology and particle size of the produced tungsten trioxide nanopowders were studied using field emission electron microscopy (FESEM). The compositional properties were investigated by using energy dispersive spectroscopy (EDS) coupled with the FESEM. The crystallite size (L, in Aº) was calculated from peak broadening using the Scherrer's approximation given in Eq. 1.

$$L = \frac{0.89\,\lambda}{B\cos\theta} \quad (1)$$

In this equation λ is the wavelength of the X-ray (1.5418 Aº), B is the full width at half maximum (FWHM, radian) and θ is the Bragg angle (degree).

3. Results and Discussion

3.1 SEM analysis

Morphological development for WO_3 nanopowders (produced using different amounts of $Na_2WO_4.2H_2O$, oxalic acid, and PEG 200), after calcination at 550ºC for 90 min, is illustrated by a series of FESEM images in Figs. 1-3. The images display a mixture of the rod-shaped or elongated sphere, regular, and sphere powders synthesized by this method. Figure 1(a, b) shows a mixture of rod-shaped and fine sphere particles produced using a minimum amount of chelating agent (32.7 mmol) and PEG (1 mmol). The average particle size is 98 nm, and the aspect ratio of the particles is calculated in the range of 1.00-4.78, which

Table 1. Summary of different preparation conditions

Sample	Precipitation condition			Resin preparation	
	$Na_2WO_4.2H_2O$(mmol)	H^+(mmol)	Number of washing steps	Oxalic acid(mmol)	PEG(mmol)
A1	12.5	125	6 (3 by 0.1 N HCl)	32.7	1
A2	12.5	125	5	49	2
A3	12.5	125	5 (by filter)	65	4
B1	25	250	7 (3 by 0.1 N HCl)	65	4
B2	25	250	5	98	8.25
B3	25	250	5 (1 by 0.1 N HCl)	131	2
C1	50	500	6	131	16.5
C2	50	500	5	196	4
C3	50	500	5 (by filter)	262	8.25

confirms the presence of rod-like morphology besides fine sphere particles. As Figure 1(e) shows the powders have a wide range of size distribution, from 40 to 200 nm. From Figure 1(a-d), it can be observed that the particles have been transformed into granular and spherical morphologies by increasing the quantity of oxalic acid and PEG. The average particle sizes reduced from 98 nm (sample A1, Figure 1(a)) to 84 nm (sample A2, Figure 1(c)) when the amount of chelating agent and PEG increased from 32.7 and 1 mmol to 49.2 and 2 mmol, respectively. Furthermore, particles with the sizes of 40-130 nm and an average aspect ratio of about 1.18 are inferred from Figure (f) for the sample A2, which concedes morphology evaluation in the sample A2 compared to the sample A1.

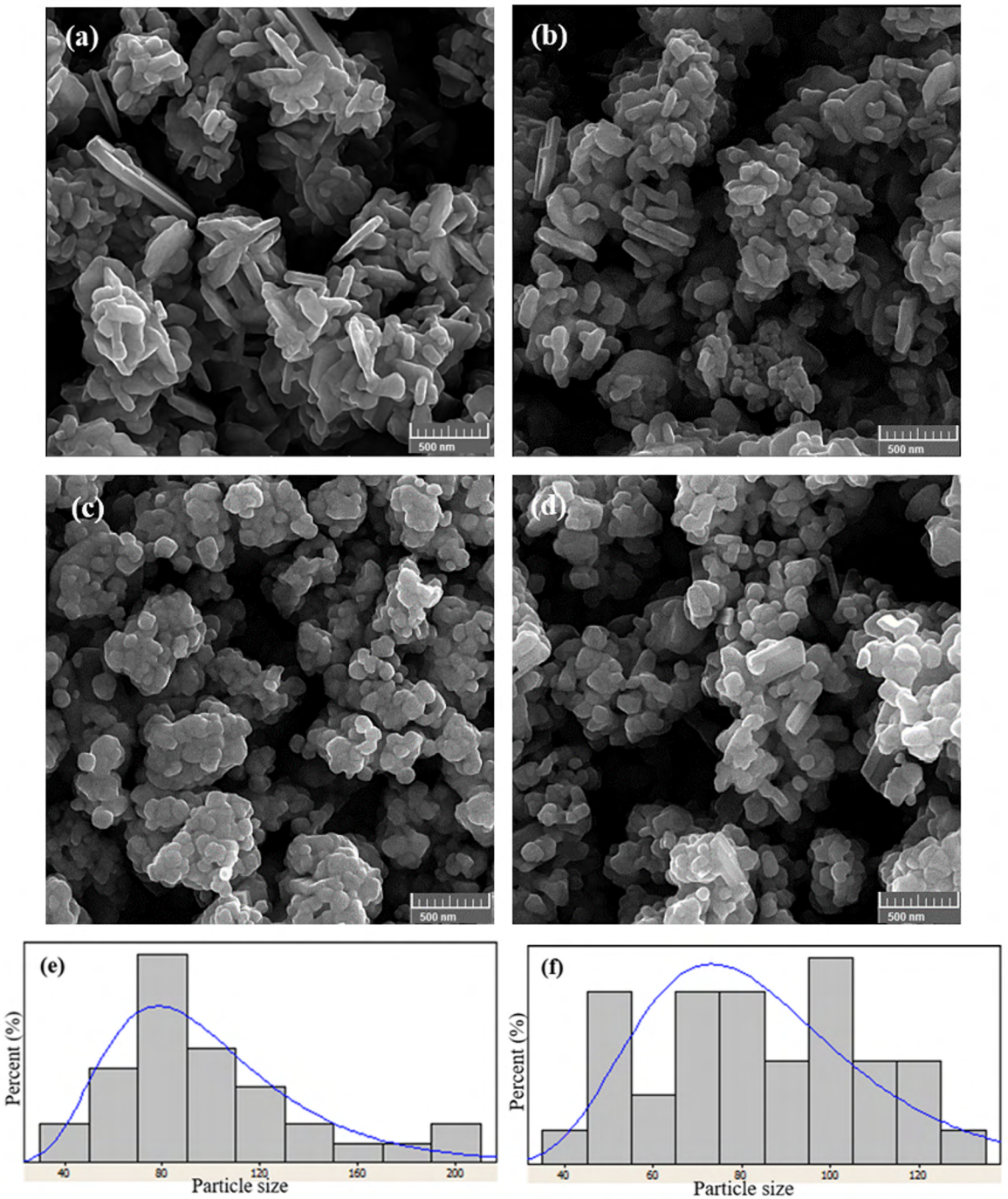

Figure 1. FESEM images of A1, A2 and A3 samples with different amount of oxalic acid and PEG: (a) and (b) 32.7 and 1; sample A1, (c) 49 and 2; sample A2, and (d) 65 and 4 mmol; sample A3, respectively; (e) and (f) particle size distribution for Figure 1(b) and Figure 1(c), respectively

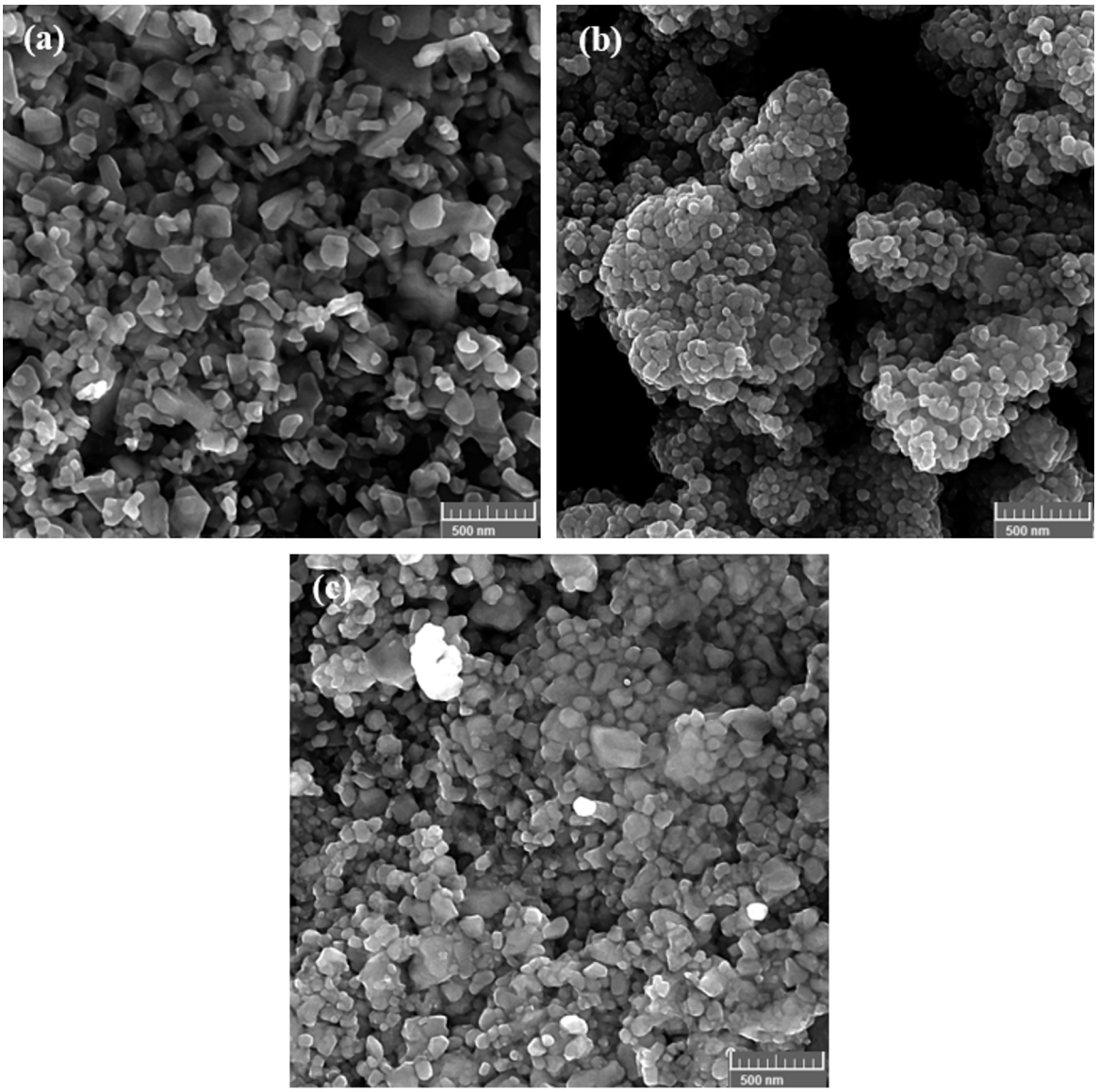

Figure 2. FESEM images of B1, B2 and B3 samples with different amount of oxalic acid and PEG: (a) 65 and 4, (b) 98 and 8.25, and (c) 131 and 2 mmol, respectively.

Further increase in the additives did not lead to apparent changes in shape and size of the particles, but it seems some particles possess regular form, as illustrated in Figure 1(d). It is worth noting that oxalic acid chelates metal cations, allowing a homogenous distribution of the cations through the polymeric chains, or reacting with the alcohol functions of the polyhydroxyl alcohol to form organic esters. Thus, when the oxalic acid increases, the quantity of hydroxyl carboxylic acid which can react with polyhydroxyl alcohol increases[11]. Oxalate anions $[(C_2O_4)^{2-}]$ as a member of dicarboxylic acid groups have been shown more effective complexing agents than the acetate anions as the monofunctional acids[16]. Oxalic acid has a better complexing effect than citric acid as well[15]. In terms of chemical structure, the chelating agents bind with $H_2WO_4.2H_2O$ [or $W(OH)_6$] and exchange with the OH^- ligands attached to the central atom, and in the case of oxalic acid, the oxalate anion strongly binds with the central W atom through bidentate ligands, as illustrated in Reaction 1[17].

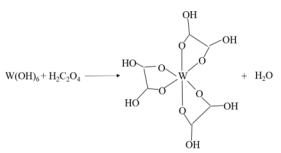

Reaction 1

This strong hydrogen bonding with the carboxyl of oxalic acid, makes WO_3 colloid particles segregate from each other and inhibits the condensation and growth of individual particles[18]. The complex formation between

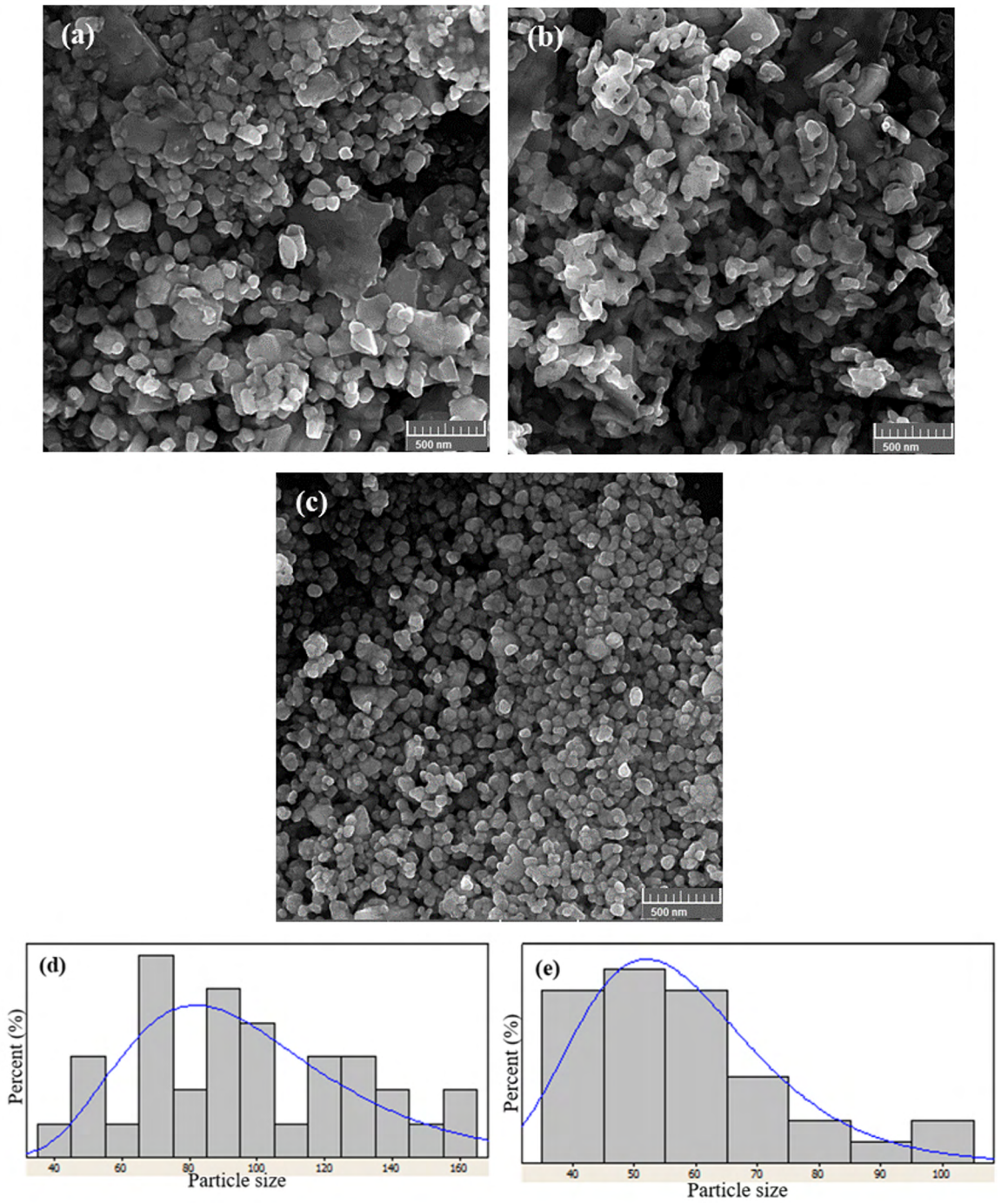

Figure 3. FESEM images of the powders prepared using different amounts of oxalic acid and PEG; (a) 131 and 16.5 (sample C1); (b) 196 and 4 (sample C2), and (c) 262 and 8.25 mmol (sample C3), respectively; (d) and (e) particle size distribution for Figure 3(a) and Figure 3(c), respectively

tungsten species and carboxylic acids are known[15,19-21]. In the presence of the complexing agent, it is expected that growth of particles stops in all directions and powders with a spherical morphology are obtained. But it can be seen that powders with rod-shaped morphology have earned in sample A1 (Figure 1 (a and b)), suggesting a different result. Patil[20] reported achieving nanorods of WO_3 by the addition of oxalic acid during hydrothermal reaction. Selectively binding of the carboxylic acid with the particular facets of the newly formed tungsten oxide hydrate seed particles is considered as the reason for this phenomenon. It leads to the stabilization of specific planes and sometimes limits the growth.

Meanwhile, some other crystallographic facets continue to grow in different particular directions to achieve rod-shaped particles eventually. Figure 2(a-c) presents FESEM images showing the particles corresponding to the samples B1, B2 and B3 prepared based on the preparation conditions given in Table 1. Regular-shaped and fine particles (Figure 2(a)) were transformed to approximately spherical-shaped particles with a uniform size as seen in Figure 2(b). In addition, as Figure 2(b) shows, particles prepared under the conditions corresponding to that of sample B2 (Table 1), agglomerated to a large size particle. Changing oxalic acid and PEG contents from 98 and 8.25 to 131 and 2 mmol, respectively resulted in the formation of almost fine regular and spherical particles as shown in Figure 2(c). It can certainly be concluded that the morphology of final powders has been affected by the quantity of both the oxalic acid and PEG.

Figure 3(a-c) shows the particles with different morphologies produced using the conditions corresponding to those of samples C1, C2, and C3. Figure 3(a) exhibits the particles with regular and spherical morphologies obtained using 131 and 16.5 mmol oxalic acid and PEG, respectively. As Figure 3(d) shows the size of particles is distributed between 40-160 nm and it can be seen that the presence of larger particles caused lack of uniformity in the particle size distribution. Figure 3(b) demonstrates elongated curved spheres along with a few large particles synthesized using the preparation condition corresponding to that of sample C2. The aspect ratio of the particles is in the range of 1.04-4.10, and the average of 2.69 supports the morphology observations. But, in a completely different FESEM image shown in Figure 3(c), spherical shape particles with a uniform size distribution were obtained.

Moreover, the particle size distribution, shown in Figure 3(e), revealed that powders with an average size less than 100 nm were obtained. The average particle size of 58 nm was measured for the this sample which are lower than what reported by Han et al.[15]. It should be noted that all samples were prepared in the presence of 50 mmol sodium tungstate while the quantity of oxalic acid (from sample C1 to C3) was increasing. This result suggests that morphology of the final powders has been affected by both the oxalic acid and PEG quantities. Considering the conditions given in Table 1, and the comparison made between FESEM images of the samples series A to C, it can be concluded that although there was a similar strategy in preparation procedure, particles with different morphologies were obtained due to the variation in PEG content. For instance, in A1, B1, and C1 samples with 32.7, 65, and 131 mmol oxalic acid, respectively, increasing PEG content from 1 to 16.5 mmol resulted in breaking the large particles down. However, there was still large particles caused lack of uniformity in size distribution, in addition to dissimilarity in the morphology of particles. On the other hand, in samples A3, B3, and C3 with 65, 131, and 262 mmol oxalic acid, respectively, the particles produced using 8.25 mmol PEG led to a uniform size distribution as well as spherically shaped particles. PEG is a short-chain polymer with a uniform and ordered chain structure, which can be easily adsorbed on the surface of metal oxide colloid. This strong interaction kinetically decreases the activities of metal oxide colloid, and thus control the growth rates of various crystallographic facets of crystals which can control the morphology[22-25]. In this research, regular and spherical particles were obtained at low and high concentrations of PEG (in all A, B, and C sample series), respectively. This corresponds to the fact that the short-chain polymer, PEG, confines the growth rate of the metal oxide colloid in some certain facet at low concentration which finally leads to an anisotropic growth of the crystals. It is found that an enough PEG concentration can confine the growth rate of the colloids in all directions which leave a spherical morphology. In another aspect of view, the formation of oligomers through polyesterification reactions which is obtained by Pechini's method, can decrease ion segregation and finally control the morphology of particles[26]. From these conclusions, it can be restated that the morphology of powder produced in this experiment depends on the quantity of oxalic acid and PEG as well as the ratios of them.

3.2 Structure analysis

Figure 4 shows a spectrum corresponding to the sample C3 obtained from EDS analysis. It reveals that the powder dominates in W and O elements. Moreover, no impurity originating from carbon additives can be seen in the spectrum.

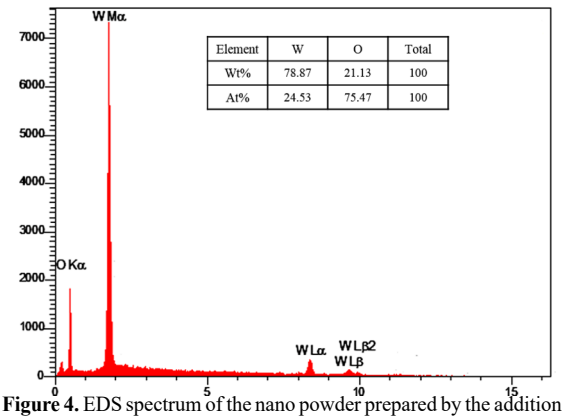

Figure 4. EDS spectrum of the nano powder prepared by the addition of 262 mmol oxalic acid and 8.25 mmol PEG to the gel and heating at 550 ºC for 90 min.

Figure 5 shows XRD patterns of the samples C1, C2, and C3 prepared by 50 mmol sodium tungstate and 500 mmol tungstic acid with different quantities of oxalic acid and EPG. The XRD patterns show that the products were crystallized in the form of a monoclinic lattice (JCPDS card 83-0950)[27,28]. The patterns indicate no considerable apparent difference between the peaks suggesting no significant dissimilarity between the powders synthesized in the samples.

No characteristic diffraction peaks from impurities were detected. In addition, the sharp and strong peaks in all the three products signify the synthesis of high crystallized powders. This confirms the relationship between crystallinity and peak intensity or sharpness that has been mentioned in some references[29,30]. Similar results from the structure, purity, and crystallinity viewpoints were obtained for the samples A and B. Therefore, in order to avoid lengthening the paper with no significant results, no similar discussions were done for them. When the amount of oxalic acid is the highest (sample C3) -relative to sample C1 and C2- the peak intensity is at the maximum value, while when the amount of PEG is the lowest (sample C2) -relative to sample C1 and C3- the peak intensity is at the minimum value. This proposes that both chelating agent and PEG along with their concentrations only affect the crystallinity of final powder in Pechini's method.

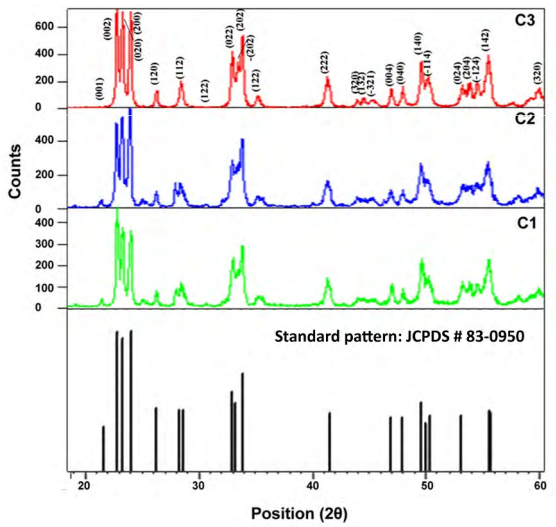

Figure 5. XRD patterns of WO_3 nano powders after calcination at 550ºC for 90 min with different amounts of oxalic acid and PEG. All peaks match with the standard pattern of monoclinic WO_3 (JCPDS # 83-0950).

The crystallite sizes were found to be 41, 33, and 39 nm for the samples C1, C2, and C3, respectively. Hence, it can be concluded that the additives amount also influences the crystallite size. On the other hand, although there is no apparent difference between the XRD patterns of WO_3 powders synthesized at different preparation condition, a product with various morphologies was obtained as well. Table 2 summarizes these results. Based on previous studies[21,31] and results obtained from this paper, it is clear that organic additive such as oxalic acid and PEG play an important role in controlling the morphology and particle size uniformity of the final products. In the present sol-gel procedure, the simultaneous presence of oxalate ion and PEG chains with different inhibitory mechanisms are able to control the size and morphology of tungsten trioxide particles at the different preparation steps.

Oxalic acid species are thermally stable up to 300ºC[32]. The presence of coordinated oxalate at the elevated temperatures can inhibit the aggregation of particles during the calcination step as well as the aqueous medium. On the other hand, oxalic acid acts as an organic fuel within thermal treatment[21]. Upon calcination in the air, oxalic acid is oxidized to carbon dioxide subsequently, and a significant amount of gases are released during the calcination step, preventing particles from continued growth and helping large agglomerated particles to break down[20,21]. In addition, the quantity of it should be controlled because of it is effective on the yield of synthesis. As expected, nanopowders synthesized by this procedure were stoichiometric WO_3 without any impurity. The organic additives (oxalic acid and PEG 200) with different quantities only acts as a crystallinity controller and never involve in changing the crystalline structure. In addition to oxalic acid, PEG with a different mechanism controls the growth of particles too. Hydrogen bonding formation between hydroxyl group in PEG and hydrogen ion in WO_3. H_2O molecule resulting in a highly unstable intermediate product (WO_3.OH-H-[$OCH_2CH_2]_n$) and H_2O. In acidic condition, this product reduced to WO_3.H_2O and PEG and

Table 2. Characterization of the product under various conditions

Sample	Product of preparation			
	XRD Guinier	Color	Crystallite size (nm)	Morphology
A1	-	Yellow	-	Regular, Rod-like
A2	-	Yellow	-	Spheres
A3	-	Yellow	-	Spheroids
B1	-	Yellow	-	Regular
B2	-	Yellow	-	Spheres
B3	-	Yellow	-	Regular, Spheroids
C1	WO_3	Yellow	41	Regular, Spheroids
C2	WO_3	Yellow	33	Regular, Curved rods
C3	WO_3	Yellow	39	Spheres

finally prevails in the growth environment. The process continues until the crystallite reaches its maximum size. The result shows that the oxalic acid and PEG concentration has a strong effect on the particle size and morphology of tungsten trioxide nanopowders. In the presence of polymeric chains of PEG, the crystal nuclei of WO_3 surrounded by this chains prevent their growth and generates the steric impediment effect leading to a reduced particle-particle aggregation[33].

4. Conclusions

In the present work, WO_3 nanopowders were successfully synthesized using the sol-gel modified Pechini's method with the aid of sodium tungstate, oxalic acid, and PEG-200 as the starting material, chelating agent, and polymeric additive, respectively. WO_3 nanopowders with a high purity, and a controllable morphology and particle size attained. The quantity of oxalic acid and PEG in the precursor, have noticeable effects on the particle shape, size, and aggregation. Nanoparticles with high crystallinity obtained via the simple and low-cost sol-gel modified Pechini's method. Particles with an average size of 58 nm and spherical morphology were synthesized by changing the amount of oxalic acid and poly ethylene glycol at the same time.

5. Acknowledgments

The authors are thankful to Iran Nanotechnology Initiative Council (Grant No. 93379) for the financial support and the Faculty of Mechanical Engineering, Shahid Rajaee Teacher Training University (SRTTU) for providing facilities. In addition, the authors would like to appreciate Eng. Ali Jafari for his very helpful assistance in conducting the experiments.

6. References

1. Campos RDC, Cestarolli DT, Mulato M, Guerra EM. Comparative Sensibility Study of WO_3 ph Sensor Using EGFET and Ciclic Voltammetry. *Materials Research*. 2015;18(1):15-19.

2. Mirzaei A, Janghorban K, Hashemi B, Neri G. Metal-core@ metal oxide-shell nanomaterials for gas-sensing applications: a review. *Journal of Nanoparticle Research*. 2015;17:371.

3. Wu CL, Wang CK, Lin CK, Wang SC, Huang JL. Electrochromic properties of nanostructured tungsten oxide films prepared by surfactant-assisted sol-gel process. *Surface and Coating Technology*. 2013;231:403-407.

4. Estupinan Donoso AA, Peters B. XDEM employed to predict reduction of tungsten oxide in a dry hydrogen atmosphere. *International Journal of Refractory Metals and Hard Materials*. 2015;49:88-94.

5. Zheng H, Ou JZ, Strano MS, Kaner RB, Mitchell A, Kalantar-zadeh K. Nanostructured Tungsten Oxide - Properties, Synthesis, and Applications. *Advanced Functional Materials*. 2011;21(12):2175-2196.

6. Won CW, Nersisyan HH, Won HI, Lee JH. Refractory metal nanopowders: Synthesis and characterization. *Current Opinion in Solid State and Materials Science*. 2010;14(3-4):53-68.

7. Al-Resheedi A, Alhokbany NS, Mahfouz RM. Radiation induced synthesis of in_2o_3 nanoparticles - part 1: synthesis of in_2o_3 nanoparticles by sol-gel method using un-irradiated and γ-irradiated indium acetate. *Materials Research*. 2014;17(2):346-351.

8. Lin J, Yu M, Lin C, Liu X. Multiform Oxide Optical Materials via the Versatile Pechini-Type Sol-Gel Process: Synthesis and Characteristics. *The Journal of Physical Chemistry C*. 2007;111(16):5835-5845.

9. Majedi A, Abbasi A, Davar F. Green synthesis of zirconia nanoparticles using the modified Pechini method and characterization of its optical and electrical properties. *Journal of Sol-Gel Science and Technology*. 2016;77(3):542-552.

10. Sakka S, ed. *Handbook of Sol-Gel Science and Technology. 1. Sol-Gel Processing*. New York: Springer; 2005.

11. Laberty-Robert C, Ansart F, Castillo S, Richard G. Synthesis of YSZ powders by the sol-gel method: surfactant effects on the morphology. *Solid State Sciences*. 2002;4(8):1053-1059.

12. Susanti D, Haryo NS, Nisfu H, Nugroho EP, Purwaningsih H, Kusuma GE, et al. Comparison of the morphology and structure of WO_3 nanomaterials synthesized by a sol-gel method followed by calcination or hydrothermal treatment. *Frontiers of Chemical Science and Engineering*. 2012;6(4):371-380.

13. Hariharan V, Radhakrishnan S, Parthibavarman M, Dhilipkumar R, Sekar C. Synthesis of polyethylene glycol (PEG) assisted tungsten oxide (WO_3) nanoparticles for L-dopa bio-sensing applications. *Talanta*. 2011;85(4):2166-2174.

14. Wang W, Pang Y, Hodgson SNB. XRD studies of thermally stable mesoporous tungsten oxide synthesised by a templated sol-gel process from tungstic acid precursor. *Microporous and Mesoporous Materials*. 2009;121(1-3):121-128.

15. Han Y, Qiu T, Song T. Preparation of Ultrafine Tungsten Powder by Sol-Gel Method. *Journal of Materials Science and Technology*. 2008;24(5):816-818.

16. Bevan J, Savage D. The effect of organic acids on the dissolution of K-feldspar under conditions relevant to burial diagenesis. *Mineralogical Magazine*. 1989;53:415-425.

17. Lu Z, Kanan SM, Tripp CP. Synthesis of high surface area monoclinic WO_3 particles using organic ligands and emulsion based methods. *Journal of Materials Chemistry*. 2002;12(4):983-989.

18. Sun M, Xu N, Cao Y, Yao J, Wang E. Nanocrystalline Tungsten Oxide Thin Film: Preparation, Microstructure, and Photochromic Behavior. *Journal of Materials Research*.2000;15(4):927-933.

19. Nayak AK, Lee S, Choi YI, Yoon HJ, Sohn Y, Pradhan D. Crystal Phase and size-Controlled Synthesis of Tungsten Trioxide Hydrate Nanoplates at Room Temperature: Enhanced Cr(VI) Photoreduction and Methylene Blue Adsorption Properties. *ACS Sustainable Chemistry & Engineering*. 2017;5(3):2741-2750.

20. Patil VB, Adhyapak PV, Suryavanshi SS, Mulla IS. Oxalic acid induced hydrothermal synthesis of single crystalline

tungsten oxide nanorods. *Journal of Alloys and Compounds*. 2014;590:283-288.

21. Hao YJ, Lai QY, Lu JZ, Wang HL, Chen YD, Ji XY. Synthesis and characterization of spinel $Li_4Ti_5O_{12}$ anode material by oxalic acid-assisted sol-gel method. *Journal of Power Sources*. 2006;158(2):1358-1364.

22. Gözüak F, Köseoglu Y, Baykal A, Kavas H. Synthesis and characterization of $CoxZn_{1-x}Fe_2O_4$ magnetic nanoparticles via a PEG-assisted route. *Journal of Magnetism and Magnetic Materials*. 2009;321(14):2170-2177.

23. Zhang DE, Zhang XJ, Ni XM, Zheng HG, Yang DD. Synthesis and characterization of $NiFe_2O_4$ magnetic nanorods via a PEG-assisted route. *Journal of Magnetism and Magnetic Materials*. 2005;292:79-82.

24. Kavas H, Baykal A, Toprak MS, Köseoglu K, Sertkol M, Aktas B. Cation distribution and magnetic properties of Zn doped $NiFe_2O_4$ nanoparticles synthesized by PEG-assisted hydrothermal route. *Journal of Alloys and Compounds*. 2009;479(1-2):49-55.

25. Köseoglu Y, Baykal A, Toprak MS, Gözüak F, Basaran AC, Aktas B. Synthesis and characterization of $ZnFe_2O_4$ magnetic nanoparticles via a PEG-assisted route. *Journal of Alloys and Compounds*. 2008;462(1-2):209-213.

26. Niederberger M, Garnweitner G. Organic Reaction Pathways in the Nonaqueous Synthesis of Metal Oxide Nanoparticles. *Chemistry A: European Journal*. 2006;12(28):7282-7302.

27. Tong PV, Hoa ND, Quang VV, Duy NV, Hieu NV. Diameter controlled synthesis of tungsten oxide nanorod bundles for highly sensitive NO_2 gas sensors. *Sensors and Actuators B: Chemical*. 2013;183:372-380.

28. Ng CY, Razak KA, Lockman Z. WO_3 nanorods prepared by low-temperature seeded growth hydrothermal reaction. *Journal of Alloys and Compounds*. 2014;588:585-591.

29. Oh JM, Hwang SH, Choy JH. The effect of synthetic conditions on tailoring the size of hydrotalcite particles. *Solid State Ionics*. 2002;151(1-4):285-291.

30. Costantino U, Marmottini F, Nocchetti M, Vivani R. New Synthetic Routes to Hydrotalcite-Like Compounds - Characterisation and Properties of the Obtained Materials. *European Journal of Inorganic Chemistry*. 1998;1998(10):1439-1446.

31. Tshabalala MA, Dejene BF, Swart HC. Synthesis and characterization of ZnO nanoparticles using polyethylene glycol (PEG). *Physica B: Condensed Matter*. 2012;407(10):1668-1671.

32. Crossey LJ. Thermal degradation of aqueous oxalate species. *Geochimica et Cosmochimica Acta*. 1991;55(6):1515-1527.

33. Wang X, Wang M, Song H, Ding B. A simple sol-gel technique for preparing lanthanum oxide nanopowders. *Materials Letters*. 2006;60(17-18):2261-2265.